

Article

Influence of Oxidation Temperature on the Regeneration of a Commercial Pt-Sn/Al₂O₃ Propane Dehydrogenation Catalyst

Chao Zhang ¹, Mingliang Tao ¹, Zhijun Sui ^{1,*} , Nihong An ², Yafeng Shen ^{2,*} and Xinggui Zhou ¹

¹ State Key Laboratory of Chemical Engineering, East China University of Science and Technology, 130 Meilong Road, Shanghai 200237, China; xgzhou@ecust.edu.cn (X.Z.)

² Sino-Platinum Industrial Catalyst (Yunnan) Co., Ltd., Yuxi 651100, China; annh@ipm.com.cn

* Correspondence: zhjsui@ecust.edu.cn (Z.S.); shenyf@ipm.com.cn (Y.S.)

Abstract: In the propane dehydrogenation process, the structure and catalytic performance stability of the catalyst are determined by its regeneration process, which includes oxidation of coke and oxychlorination to redisperse the supported metal particles. A commercial Pt-Sn catalyst was used in this work to investigate the impact of oxidation temperature on oxychlorination performance. The catalysts after oxidation and oxychlorination were characterized by H₂-TPR, CO-DRIFTS, HAADF-STEM, XPS, and CO chemisorption. It was found that mild sintering of Pt occurred during oxidation in the temperature range of 550–650 °C, and the catalyst could be fully restored in the subsequent oxychlorination treatment. Upon oxidation of the catalyst at 700 °C, a severe aggregation of Pt and SnOx could be observed, and the catalyst could not be fully regenerated under the given oxychlorination conditions. However, PDH catalyst deactivation caused by sintering is not irreversible. By tailoring the oxychlorination conditions, the detrimental effect of high oxidation temperature on regeneration could be ruled out. During the oxidation and oxychlorination treatment, the metal tends to migrate to anchor on sites with stronger metal–support interaction, which was helpful for enhancing the catalytic activity.

Keywords: propane dehydrogenation; Pt-Sn catalyst; regeneration; oxychlorination; oxidation; calcination



Citation: Zhang, C.; Tao, M.; Sui, Z.; An, N.; Shen, Y.; Zhou, X. Influence of Oxidation Temperature on the Regeneration of a Commercial Pt-Sn/Al₂O₃ Propane Dehydrogenation Catalyst. *Catalysts* **2024**, *14*, 389. <https://doi.org/10.3390/catal14060389>

Academic Editor: Zhong-Wen Liu

Received: 15 May 2024

Revised: 31 May 2024

Accepted: 7 June 2024

Published: 18 June 2024



Copyright: © 2024 by the authors. Licensee MDPI, Basel, Switzerland. This article is an open access article distributed under the terms and conditions of the Creative Commons Attribution (CC BY) license (<https://creativecommons.org/licenses/by/4.0/>).

1. Introduction

Direct dehydrogenation of propane (PDH) has become one of the most important processes for the on-purpose production of propene, an important raw material for many chemicals and polymers. Supported Pt and CrOx are the two widely used catalysts for these processes [1]. Pt-based catalysts have the advantage of high selectivity and are environmentally friendly. But PDH reaction is usually carried out at high temperature, and catalyst deactivation due to the coking problem is still inevitable [2].

In the commercial PDH process, e.g., Oleflex, a process for regeneration of the catalyst is adopted to overcome the coking deactivation problem, in which coke accumulated on the deactivated catalysts is first removed through oxidation at high temperature, typically between 450 and 600 °C [3]. The actual temperature on the catalyst surface may be even higher since coke combustion is a rapid exothermic reaction, which leads to a temperature rise of the catalyst [4]. Under high-temperature oxidation conditions, Pt metal particles on the catalyst surface are prone to sinter due to the lower melting point of PtOx than Pt. Then, subsequent oxychlorination is necessary for the regeneration process to redisperse metal particles.

The sintering of metal particles at high temperatures is one of the main causes of PDH catalyst deactivation [5]. To mitigate the consequence of sintering, a general strategy for catalyst development is to engineer the metal particles and their interactions with catalyst carriers [6]. This is also valid for developing alumina-supported Pt-based PDH catalysts. Shi et al. [7] reported that a γ -Al₂O₃ nanosheet contained a large amount of

pentacoordinate Al^{3+} , which could increase the interaction between metal and support and stabilize the Pt-Sn cluster to enhance its catalytic performance. Mironenko et al. [8] found that the surface properties of a $\gamma\text{-Al}_2\text{O}_3$, e.g., the surface bridging OH group amount and concentration of Lewis acid sites, could be altered by hydrothermal treatment and so did the metal complex-support interaction. Liu et al. [9] showed that Pt clusters are prone to sintering on $\text{Al}_2\text{O}_3(110)$ and the addition of Sn could enhance the structure stability. Regarding alumina morphology, different additives have also been used to develop sinter-resistant catalysts for PDH [10–14]. But the long-term structure stability in the reaction-regeneration cycles has been seldom verified and sintering problems may still exist under high temperatures [15].

Temperature is a key factor in controlling the aggregation of metal particles. Depending on the treatment temperature, either dispersion or sintering of Pt could occur [16,17]. Usually, oxidation under low temperatures would cause fewer sintering problems. Alcalá et al. [18] prepared supported PtMn, PtZn, and PtSn catalysts for PDH and found oxidation of the spent catalysts in air at 420 °C had minimal catalyst sintering and that their catalytic performance could be fully recovered. But the effect of temperature on sintering may be entwined with other factors, e.g., catalyst composition [19], morphology/structure [20], and treatment atmosphere [21,22]. Zhao et al. [23] found that structures of Pt-Sn/catalysts with a high Sn/Pt ratio are self-adaptive for catalyzing PDH during oxidation of the spent catalyst at 600 °C, in which Pt migrated to anchoring sites with strong interaction between Pt and the support, leading to higher dispersion of Pt and better catalytic performance. These complicated phenomena found in oxidation all originated from the mobility of the atoms under high temperatures [6,22]. Especially for the adoption of alumina as PDH support, the change in its surface and/or structure properties was almost inevitable because of the high temperature and various atmospheres of reaction, oxidation, and oxychlorination process [24].

Oxychlorination has long been known as the effective method for redispersing a sintered catalyst [25]. Some new methods for redispersing metal catalysts by using different chlorine dispersants have been reported in recent years [26,27]. The key role of oxychlorination regeneration on the long-term structure and performance stability of Pt-based PDH catalysts may lie in the fact that a steady state of Pt could be reached after long-time operation or multiple reaction-regeneration cycles, and this state is favorable for catalyzing PDH reaction [28]. The steady structure of the redispersed catalyst is a function of oxychlorination conditions and properties of the interface between the supported metal and the support [29]. Since the properties of the support, as well as the metal, could be altered during the oxidation treatment, the oxidation temperature must have an impact on the consequent oxychlorination treatment, and its influence should be carefully examined for a given PDH catalyst.

In this work, a commercial Pt-Sn/ Al_2O_3 PDH catalyst was oxidized under different temperatures to obtain samples with different degrees of sintering. Using dichloroethane (EDC) as a chlorine source, the sintered catalysts were regenerated. The effect of the oxidation temperature on the structure and catalytic performance of the catalyst after oxychlorination treatment was investigated. It was believed that the results were of significant practical value for the optimization of the process of Pt-based PDH catalyst regeneration and helpful for the development of sinter-resistant PDH catalysts.

2. Results

2.1. Catalytic Performance

The catalytic performance of the catalysts before and after regeneration is presented in Figure 1. It can be observed that within 3 h of time on stream, the conversion of the Fresh catalyst ranged from 12% to 10%, with a stable selectivity of 99.5%. Prior to regeneration, the conversion of the catalyst decreased gradually with increasing oxidation temperature when the oxidation temperature was between 550 °C and 650 °C. However, the conversion of the Sinter-700 °C dropped dramatically to less than 2%, which may be due to the aggregation

of Pt particles caused by excessively high oxidation temperature. In addition, all catalysts oxidized at different temperatures exhibited a decrease in propylene selectivity.

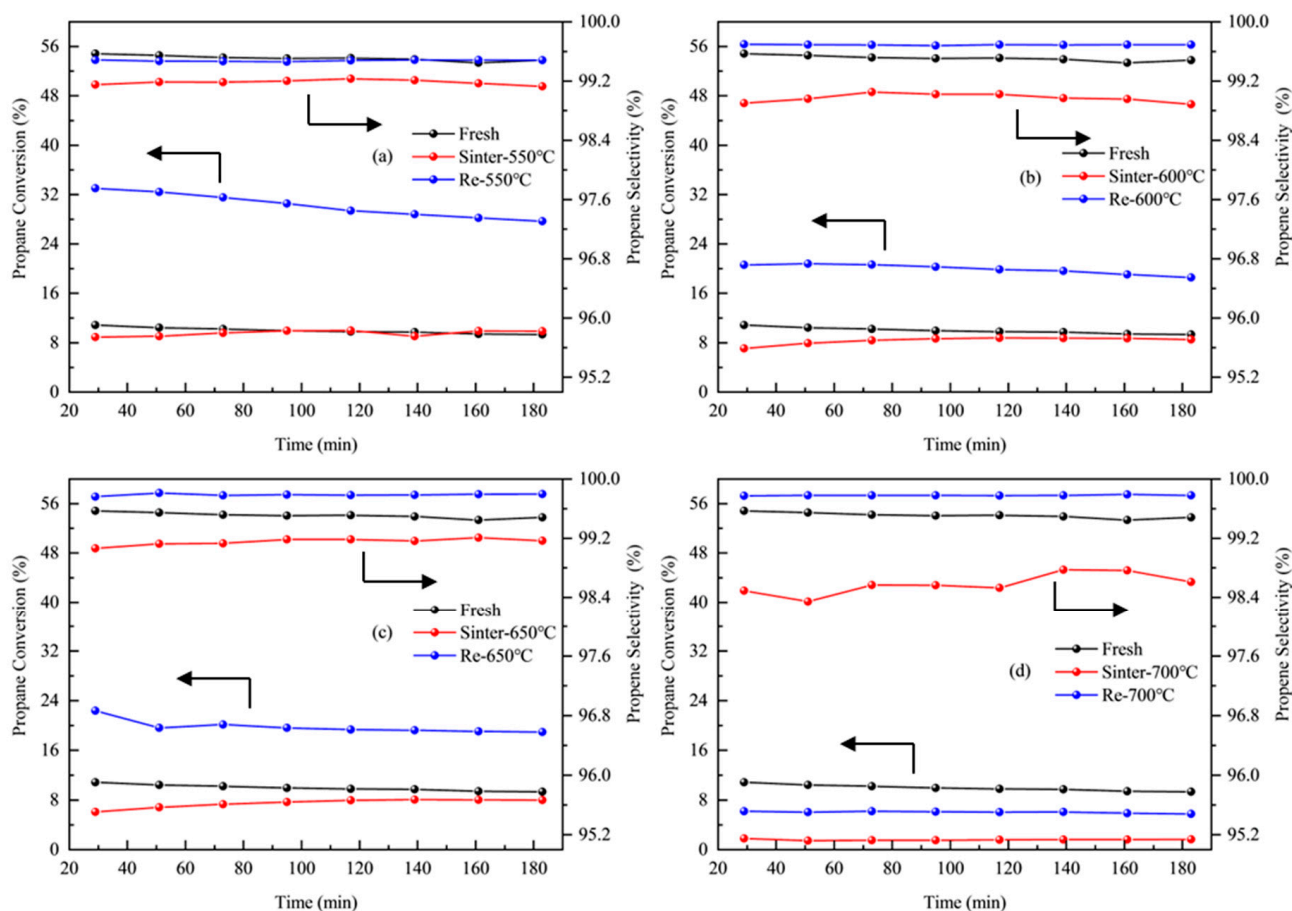


Figure 1. Catalytic performance of catalysts after calcination under different temperatures: (a) 550 °C, (b) 600 °C, (c) 650 °C, (d) 700 °C.

After regeneration, the conversion and selectivity of the four catalysts showed varying degrees of improvement. Among them, the Re-550 °C catalyst achieved the highest initial propane conversion of 34.7%. The Re-600 °C and Re-650 °C had similar initial propane conversion of around 23%, higher than the Fresh catalyst. In contrast, Re-700 °C only had a conversion of 6%, slightly higher than the Sinter-700 °C catalyst, but still lower than the Fresh catalyst, indicating that its activity could not be fully restored under these regeneration conditions. This suggested that the oxidation temperature directly affected the regeneration of the catalyst. High oxidation temperatures may hinder or prohibit the recovery of catalytic performance through the oxychlorination process, possibly due to the severe sintering of active metal. The selectivity to propylene on all the regenerated catalysts (>99.5%) is higher than that of the Fresh catalyst.

2.2. TG Results

TG was used to characterize the coke amount accumulated on the catalysts. The TG and DTG curves under an oxidative atmosphere are shown in Figure 2. The main weight loss peak centered around 475–525 °C and was due to the oxidation of cokes. Some peaks centered at lower temperatures, around 175 °C and 325 °C, can also be found on some samples, which could be ascribed to the oxidation of cokes accumulated on/near the active metals [30]. The coke amount in different samples varied with calcination temperature, although the selectivity to propylene was close in these samples. Considering different propane conversions obtained on each sample, the coking index has been introduced in

this article, defined as the ratio of the accumulated coking amount/propylene yield on a sample [30]. The results are listed in Table 1. A smaller K value indicates a lower coking selectivity. It was observed that the K values of the catalysts reached their minimum at the lowest oxidation temperature and increased with the increasing oxidation temperature, finally reaching nearly 4 times that of the Fresh catalyst. The K values of the regenerated catalysts were all lower than that of the counterpart. The change in the coking amount/coking index clearly indicated the change in catalyst structure.

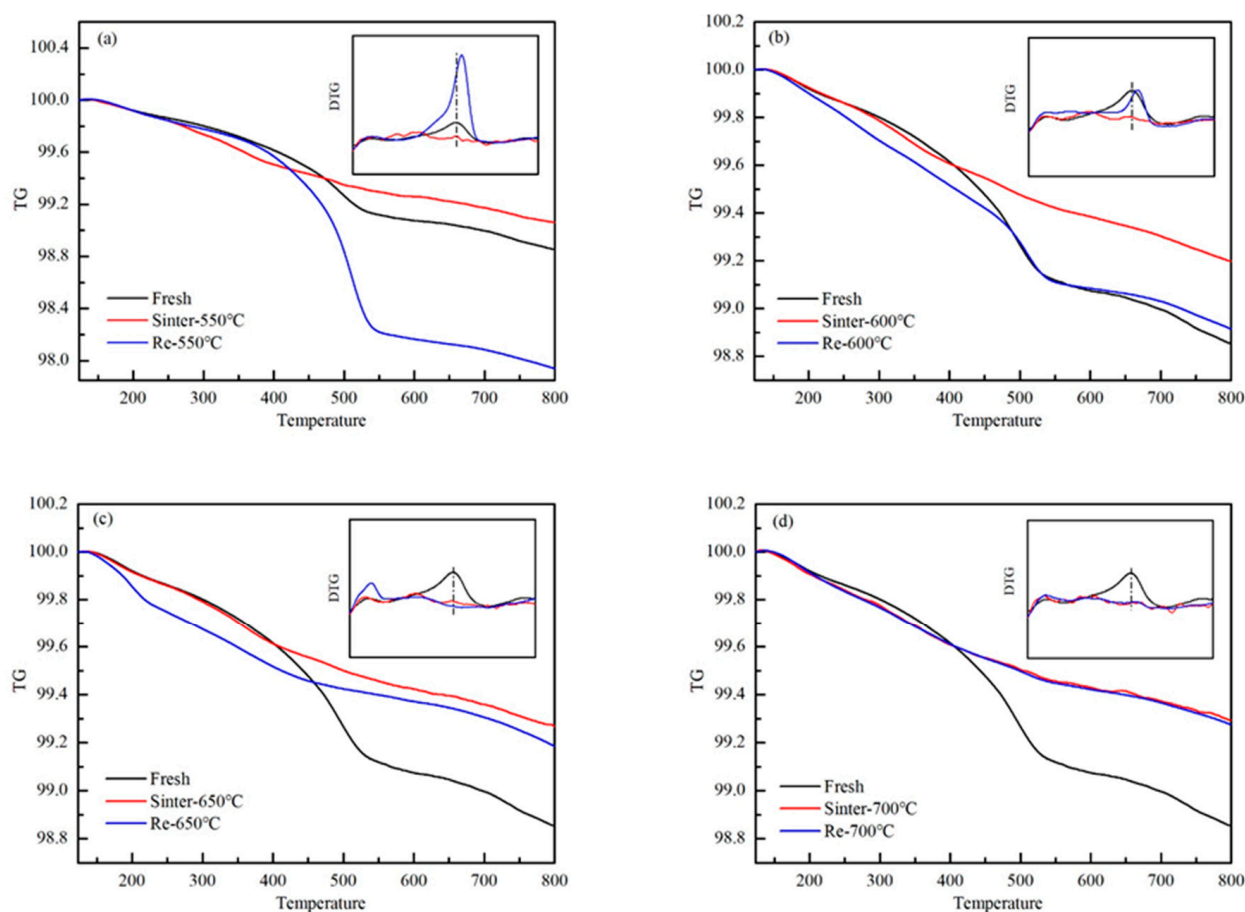


Figure 2. TG and DTG curves of the spent catalysts before and after regeneration: (a) catalyst oxidation at 550 °C, (b) catalyst oxidation at 600 °C, (c) catalyst oxidation at 650 °C, (d) catalyst oxidation at 700 °C; the vertical line indicating the peak temperature for weight loss.

Table 1. The coke index of catalysts after different treatments.

Sample	Coke Index	
	N ₂	O ₂
Fresh	0.123	0.147
Sinter-550 °C	0.087	0.084
Sinter-600 °C	0.095	0.106
Sinter-650 °C	0.092	0.105
Sinter-700 °C	0.436	0.526
Re-550 °C	0.075	0.077
Re-600 °C	0.059	0.059
Re-650 °C	0.043	0.042
Re-700 °C	0.126	0.138

The difference in coking index K obtained from the N₂ and O₂ atmosphere can be an indicator of the change in catalyst structure [30,31]. The K values obtained in the N₂ atmosphere do not include the weight loss of highly graphitic coke generated from active sites containing multiple Pt-Pt bonds. The diminishment of this difference in the K values suggests the atomically/high dispersion of Pt. Large differences in coke index obtained from different TG atmospheres could be found in Fresh, Sinter-600 °C, Sinter-650 °C, and Sinter-700 °C samples, which suggested that agglomeration of Pt atoms exists in these catalysts. Sinter-550 °C and all the samples after regeneration had close K values, indicating Pt atoms are well dispersed during the process.

2.3. N₂ Physisorption

The nitrogen physisorption characterization results are shown in Table 2. It can be observed that the catalysts exhibited a slight increase in specific surface area (90.2–95.3 m²/g), average pore diameter (26.2–28.1 nm), and total pore volume (0.62–0.67 cm³/g). After oxychlorination regeneration, the specific surface area of the catalysts decreased slightly (88.3–93.3 m²/g), while the average pore diameter and total pore volume increased slightly. These changes were minor, which demonstrated that oxidation and oxychlorination treatment has no significant impact on the textural properties of the catalyst.

Table 2. Textural properties of catalysts after different treatments.

Samples	S _{BET} (m ² /g)	D _{pore} (nm)	V _{pore} (m ³ /g)
Fresh	90.1	27.6	0.62
Sinter-550 °C	90.2	26.2	0.59
Sinter-600 °C	92.5	27.5	0.63
Sinter-650 °C	93.0	27.5	0.64
Sinter-700 °C	95.3	28.1	0.67
Re-550 °C	88.3	27.9	0.62
Re-600 °C	87.5	28.8	0.63
Re-650 °C	89.3	29.1	0.65
Re-700 °C	93.3	28.8	0.67

2.4. H₂-TPR

The H₂-TPR characterization results are shown in Figure 3. Two peaks, a weak peak around 230–280 °C, and a strong broad peak extending from 450–650 °C can be observed. The low-temperature reduction peak was attributed to the reduction in oxidized platinum species weakly interacting with support [32] or Sn oxide catalyzed by Pt [33]. Lieske [34] also reported a reduction peak of [Pt^{IV}(OH)_xCl_y]_s centered around 270 °C, which may be formed during the preparation or oxychlorination regeneration process. But this peak could be found in samples after oxychlorination treatment. The high-temperature reduction peak was attributed to the reduction in SnO_x species from Sn⁴⁺ to Sn²⁺ and Sn²⁺ to Sn⁰ [35,36].

After oxidation treatment at different temperatures, the high-temperature reduction peaks of the catalysts shifted towards higher temperatures and the peak width became narrower, which suggested that the metal species were redispersed and anchored on sites with stronger metal–support interaction during the process. After oxychlorination regeneration, the positions of the sole reduction peaks for the four catalysts were 561 °C, 573 °C, 578 °C, and 590 °C, respectively. Compared with the Fresh and the counterpart Sinter samples, the peak positions shifted towards higher temperatures with the increasing oxidation temperature. Meanwhile, the shoulder of the peak became more ambiguous and the peak for Re-700 °C became almost symmetric. It also should be noted that the peak temperature of the low-temperature reduction peak shifted higher when the oxidation treatment temperature was increased. These findings indicate that the structure of the catalyst underwent changes during the oxidation and oxychlorination regeneration process, in which the Pt and Sn species can migrate and selectively anchor on sites with stronger

metal–support interaction, leading to the disappearance of low-temperature reduction peaks and narrower SnO_x reduction peaks with higher reduction temperatures in TPR.

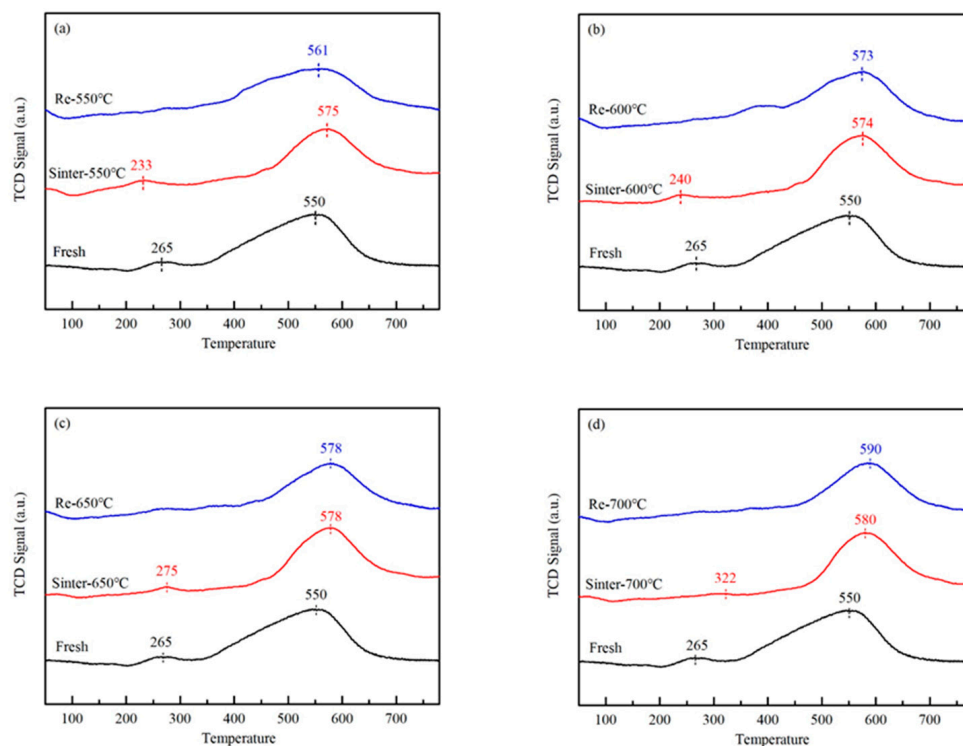


Figure 3. H₂-TPR images of catalysts after oxidation under different temperatures: (a) catalyst oxidation at 550 °C, (b) catalyst oxidation at 600 °C, (c) catalyst oxidation at 650 °C, (d) catalyst oxidation at 700 °C.

2.5. CO-DRIFTS

The CO-DRIFTS characterization results are shown in Figure 4. It can be observed that the Fresh sample exhibited two distinct adsorption bands at 2037 cm⁻¹ and 2094 cm⁻¹. It was reported that bands in the range of 2080–2095 cm⁻¹ could be attributed to CO adsorbed on ionic Pt^{δ+} species corresponding atomically dispersed Pt species, or formed by oxidation of Pt precursor during the preparation process [37]. The peak at 2037 cm⁻¹ was assigned to CO adsorption on Pt₃Sn alloys [32,38]. The addition of Sn to Pt could decrease the number of adjacent Pt atoms, leading to the reduced CO-CO dipole coupling and CO stretching frequency, and assist in the back donation of d-electrons into the 2π* orbital of CO, lowering the vibration frequency of adsorbed CO [32,39]. The peaks in the spectra of the Fresh sample appeared to be broader than those of the two other samples, which suggested that the non-uniformly distributed Pt species on the support.

After oxidation at different temperatures, the peaks at 2037 cm⁻¹ disappeared and the peaks at 2094 cm⁻¹ shifted to a lower wavenumber. The former result indicated that the Sn segregated from the Pt-Sn alloy and interacted more strongly with the support as evidenced by the TPR results. Pham et al. [40] found that the addition of Sn to an alumina-supported Pt catalyst provided the necessary nucleation sites to enhance the redispersion of Pt in the oxidative regeneration process. This also illustrated the red shift of 2094 cm⁻¹ bands, which was caused by the changing anchoring sites for Pt. Additionally, the peak heights and areas gradually decreased with the increasing oxidation temperature because more Pt surface was covered by the aggregated Sn component due to the higher oxidation temperature [41,42].

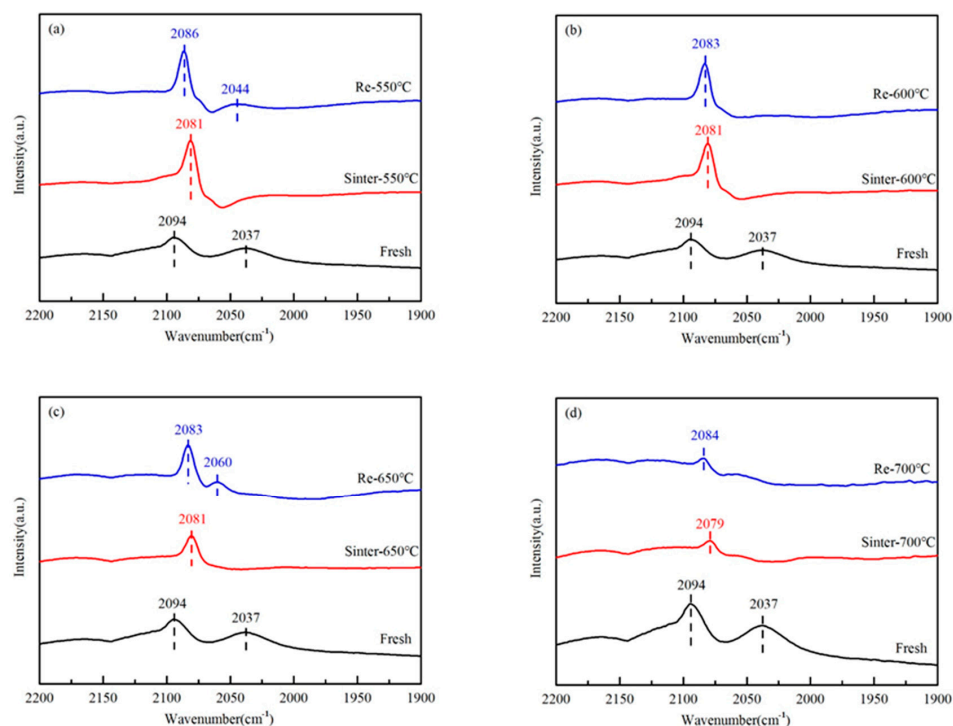


Figure 4. CO–DRIFTS spectra of catalysts before and after oxychlorination regeneration: (a) catalyst oxidation at 550 °C, (b) catalyst oxidation at 600 °C, (c) catalyst oxidation at 650 °C, (d) catalyst oxidation at 700 °C.

After oxychlorination regeneration, the bands at $\sim 2080\text{ cm}^{-1}$ exhibited a blue shift, possibly because the introduction of Cl during the oxygen–chlorine process reduced the electron density on the Pt surface in close contact with the highly electronegative Cl [43]. A band at 2044 appeared after regeneration under 550 °C and was ascribed to Pt3Sn alloy, which verified the redispersion of metal species during the process. A 2060 cm^{-1} band appeared after regeneration under 650 °C and still could be observed after 700 °C regeneration, which was due to the sintering of Pt during high-temperature oxidation and the formation of well-coordinated Pt metallic particles (refer to Figure 5).

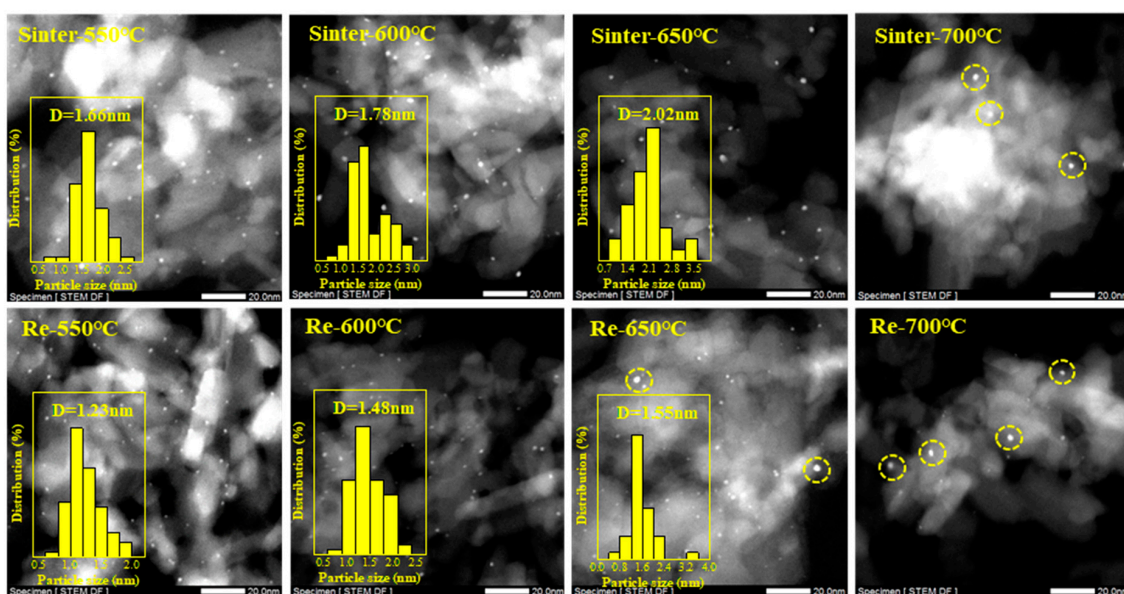


Figure 5. HAADF-STEM images and particle size distribution of different catalysts (the yellow circle indicates particles with particle size larger than 3 nm).

2.6. CO-Chem and HAADF-STEM

The dispersion and particle size distribution of Pt before and after regeneration were characterized by CO-Chem and HAADF-STEM, and the results are shown in Table 3 and Figure 5. According to Table 3, the dispersion of the Sinter catalysts was lower than that of the Fresh catalyst and gradually decreased with the increasing oxidation temperature. Statistical analysis of the metal particles using Nano Measure software version 1.2 revealed that the Sinter-550 °C catalyst had a relatively uniform distribution of particle size, with an average of 1.66 nm. When the oxidation temperature increased to 600 °C, the particles noticeably increased in size, with an average particle size of 1.78 nm and a bimodal distribution. Further oxidation to 650 °C resulted in further particle growth, with an average particle size of 2.02 nm. At 700 °C, particles in the range of 1–2 nm can hardly be observed. Instead, particles of ~3 nm and above (marked with yellow circles in the figure) in diameter could be found. Thus, different oxidation temperatures directly affected the geometric size of the Pt particles in the catalyst. Above 550 °C, higher oxidation temperatures could lead to more severe sintering of the catalyst. The gradually enlarged discrepancy between particle size determined by CO-Chem and HAADF-STEM should also be noticed, which was caused by the segregation of Sn species on Pt [38,40], according to the CO-DRIFTS results.

Table 3. Particle size and dispersion of catalysts after different treatments.

Samples	Pt Dispersion (%)	D _{CO-Chem} (nm)	D _{TEM} (nm)
Fresh	70.15	1.5	1.49 ± 0.3
Sinter-550 °C	62.88	1.6	1.66 ± 0.25
Sinter-600 °C	48.33	2.3	1.78 ± 0.13
Sinter-650 °C	35.58	3.2	2.02 ± 0.38
Sinter-700 °C	17.14	5.5	>3 nm
Re-550 °C	82.98	1.2	1.23 ± 0.21
Re-600 °C	63.57	1.6	1.48 ± 0.36
Re-650 °C	59.41	1.6	1.55 ± 0.24
Re-700 °C	19.44	4.9	2~3 nm

Both sintering and dispersion of Pt during an oxidation treatment have been reported [16,17]. From a kinetic point of view, the sintering or dispersion process is reversible [6]. Whether the metal was sintered or dispersed depended on which process was superior during the treatment [16]. Generally, low temperature (450–500 °C) and low oxidant concentration were beneficial for the dispersion process [41]. But it should be noted that the temperature for catalyst sintering is related to the catalyst composition and structures [44]. However, oxidation temperature is a key factor for maintaining the stability of the catalyst for a given catalyst, especially for catalysts without or with a low ratio of structure promoters for the dispersion of Pt. Temperatures below 550 °C were recommended for oxidation of the Pt-Sn catalyst, which could guarantee the structure stability of the catalyst.

After oxychlorination regeneration, the dispersion of the catalysts oxidized at 550 °C, 600 °C, 650 °C, and 700 °C increased to 82.98%, 63.57%, 59.41%, and 19.44%, respectively, and the calculated particle sizes were 1.20 nm, 1.57 nm, 1.62 nm, and 4.85 nm, respectively. The particle size determined from HAADF-STEM results showed that the average particle size of the catalysts after regeneration at 550 °C, 600 °C, and 650 °C were 1.23 nm, 1.48 nm, and 1.55 nm, which were well consistent with those from CO-Chem results. Among them, the catalyst oxidized at the lowest temperature (550 °C) could be fully regenerated, whose dispersion surpassed that of the Fresh catalyst. The catalysts oxidized at 600 and 650 °C could be partly recovered for their dispersions. For the catalyst regenerated at 600 °C, although most particle sizes center around 1.55 nm, there were still a few particles above 3 nm that could not be dispersed. For the Re-700 °C catalyst, it was observed that although a few particles were redispersed into small particles of 1–2 nm after regeneration, most of

the particles of 3 nm and above remained. Therefore, under the regeneration conditions used here, the oxygen–chlorine treatment had a good redispersion effect on particles in the 1–2 nm range, but was not suitable for catalysts with a large number of particles sized 3 nm and above.

2.7. XPS

XPS was used to analyze the changes in the valence states of the Pt and Sn in the sinter and Re catalysts. The results for Pt $4d_{5/2}$ orbital spectra are shown in Figure 6. It can be observed that the Fresh catalyst exhibited three characteristic peaks at 318.5 eV, 315.5 eV, and 313.0 eV, corresponding to Pt^{4+} , Pt^{2+} , and Pt^0 species, respectively. After oxidation treatment, the peak intensity of Pt gradually decreased with the increasing oxidation temperature, becoming very weak to Sinter-700 °C due to the segregation of Sn species on the Pt surface, which was consistent with the results from CO-DRIFTS. All three characteristic peaks of Pt in Sinter-700 °C migrated to lower binding energy, indicating that the high-temperature oxidation treatment could aggregate Pt metal, reduce its electron density, and increase the proportion of the Pt^0 species. Among all the four Sinter series samples, Sinter-600 °C had the highest binding energy of Pt species. This result seemed to be contradictory with results from other samples because aggregation of Pt metal generally lowers its binding energy. But it should be noted that the existence state of Sn also changed the binding energy of Pt species. From Figure 7, it can be observed that Sinter-600 °C has the lowest SnO_x/Sn ratio, indicating that part of the Sn species segregated from Pt-Sn bimetal particles and increased the binding energy of Pt.

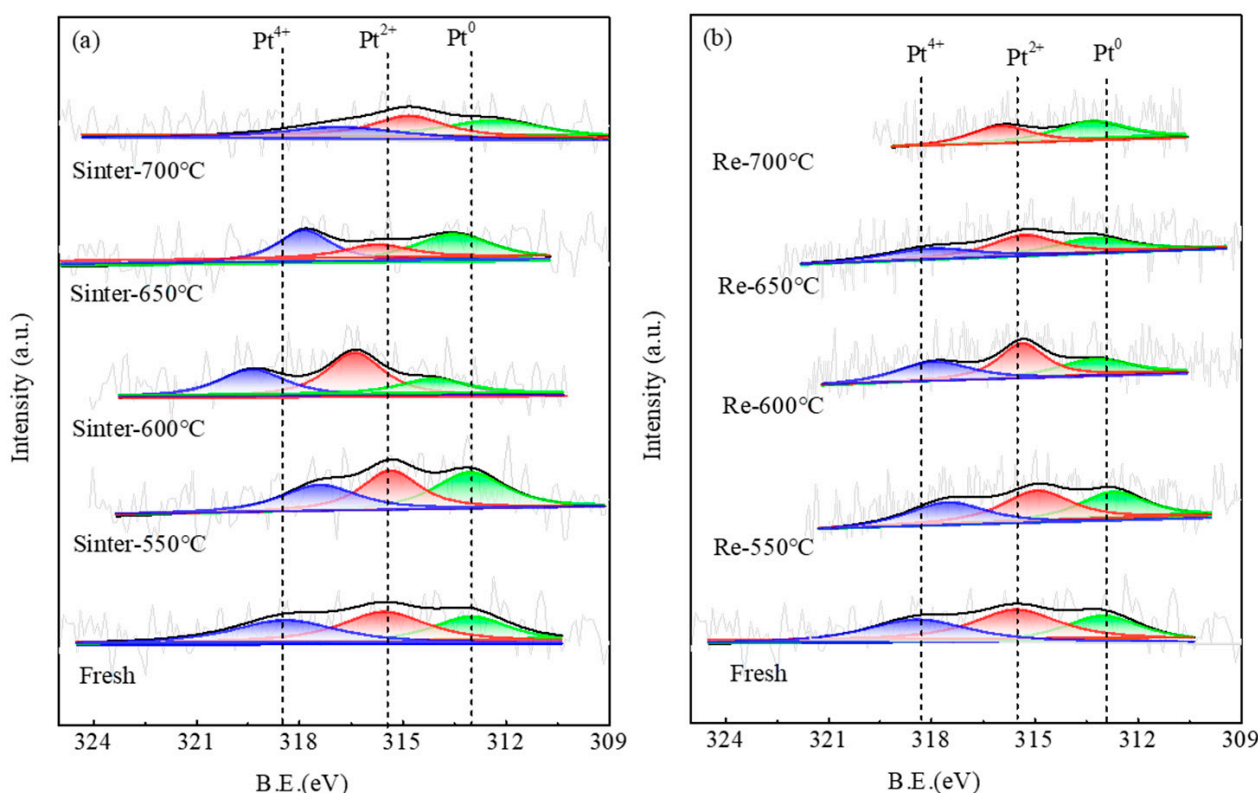


Figure 6. Pt $4d_{5/2}$ XPS spectra of catalysts with different oxidation degrees before (a) and after (b) regeneration.

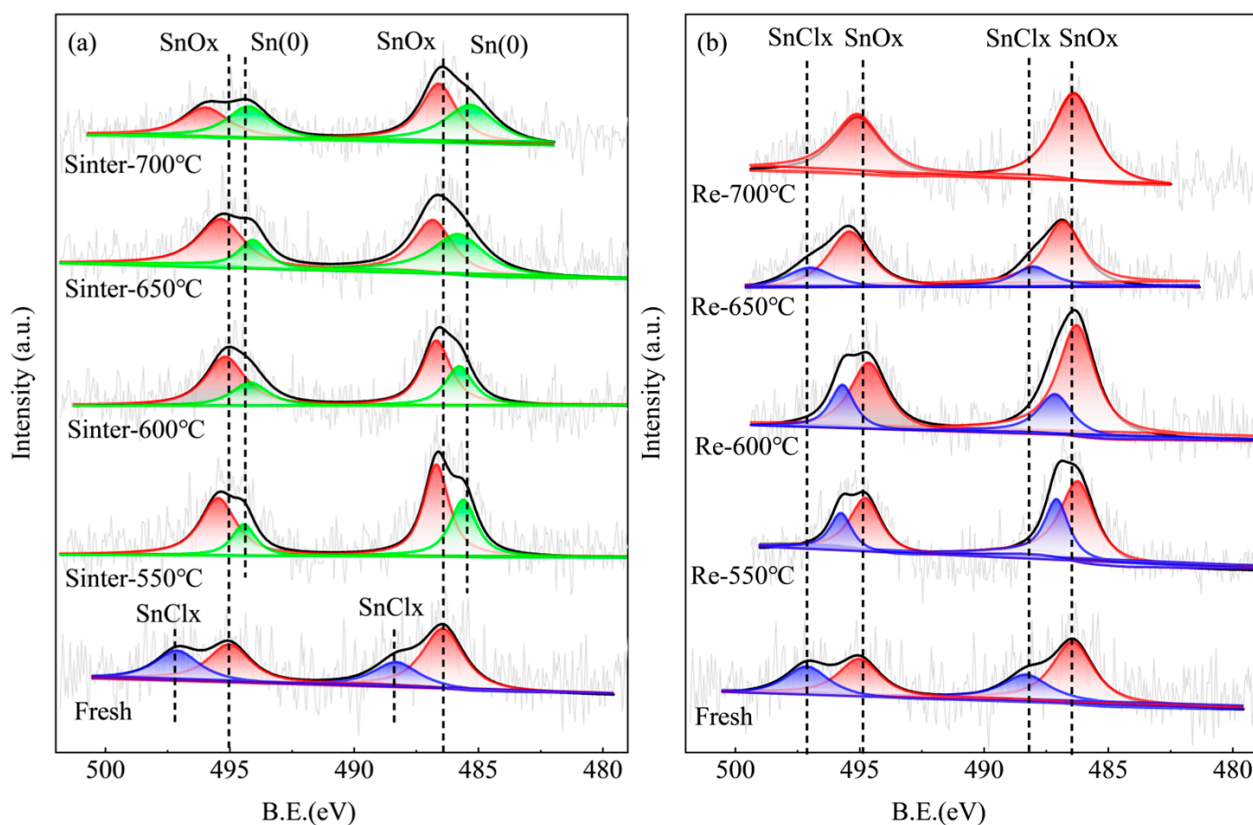


Figure 7. Sn $3d_{5/2}$ XPS spectra of catalysts with different oxidation degrees before (a) and after (b) regeneration.

The XPS spectrum of the Sn component is shown in Figure 7. The peaks of binding energy at 488.3 and 487.1 could be attributed to the Sn(IV) and Sn(II) chlorinated species, respectively [45,46]. The component at a binding energy of 486.6 eV was characterized as SnOx, either in the Sn⁴⁺ or Sn²⁺ state [47,48]. The peak at 485.2 eV was attributed to metallic Sn species. This binding energy was close to that reported by Virnovskaia et al. [48], which is slightly higher than Sn3d in a metallic state, around 484.5–484.9 eV [49], and could be ascribed to quasi-metallic Sn, resembling the O-Sn chemisorption state. For the Fresh catalyst, Sn existed in SnClx and SnOx states. During oxidation treatment at different temperatures, the Sn-Cl bond was broken, and Sn species may migrate and interact with supports and form quasi-metallic Sn, as evidenced by the shift in binding energy to higher binding energy when the oxidation temperature increased from 550 °C to 650 °C. During the oxychlorination process, the quasi-metallic Sn component disappeared and SnClx species were produced again. Special attention should be paid to the Sinter-700 °C and the following Re-700 °C sample. The peak for the quasi-metallic Sn component in Sinter-700 °C shifted to lower binding energy, close to that of metallic Sn, indicating the aggregation of Sn. After chlorination regeneration, the Sn peak for the Re-700 °C sample was symmetrical and could be well fitted by one Gaussian curve, indicating the Sn existed in SnOx species only. The disappearance of the SnClx peak suggests that the aggregation of Sn in 700 °C oxidation hindered the formation of SnClx and the promoter effect on the redispersion of Pt was weakened.

2.8. Optimization of Oxychlorination Conditions

As stated above, when the catalyst was oxidized at a high temperature of 700 °C, the performance of the catalyst after regeneration, Re-700 °C, was extremely poor due to the bad redispersion of Pt and segregation of Sn. This indicates that the oxychlorination conditions may not be suitable to achieve a full restoration of the catalyst structure or that

the catalyst deactivation was irreversible through the oxychlorination regeneration process. Then, attempts were made to explore the potential to recover the catalyst activity under conditions different from those stated in Section 3.

In the experiment, the regeneration temperature, oxygen concentration, chlorine concentration, and regeneration time were changed. The performance of these regenerated catalysts is shown in Figure 8. It was found that, compared with other factors, oxychlorination temperature had a major influence on the regeneration of Sinter-700 °C. The best initial propane conversion could reach 12.0% on the Re2-530 °C catalyst, which is close to the Fresh catalyst, when the regeneration temperature increased to 530 °C. But the activity of the Re2-530 °C catalyst decreased more rapidly than the Fresh catalyst during 3 h of reaction and far below those for Re-550 °C and Re-600 °C. Moreover, when the regeneration time is increased to 60 min, the initial propane conversion can only reach 10.8% and declines to only 5% after 3 h of reaction. These results indicated that the deactivation of the catalyst under 700 °C oxidation was not totally irreversible. By tailoring oxychlorination conditions to accelerate the redispersion rate, the catalyst structure could be partly restored after a certain time. This also indicated that the control of the oxidation temperature during the coke-burning process had a significant impact on the regeneration performance. When the catalyst was oxidized at different temperatures, the oxychlorination conditions should be tailored to favor its redispersion kinetics, as well as thermodynamic equilibrium state, for maximizing regeneration efficiency.

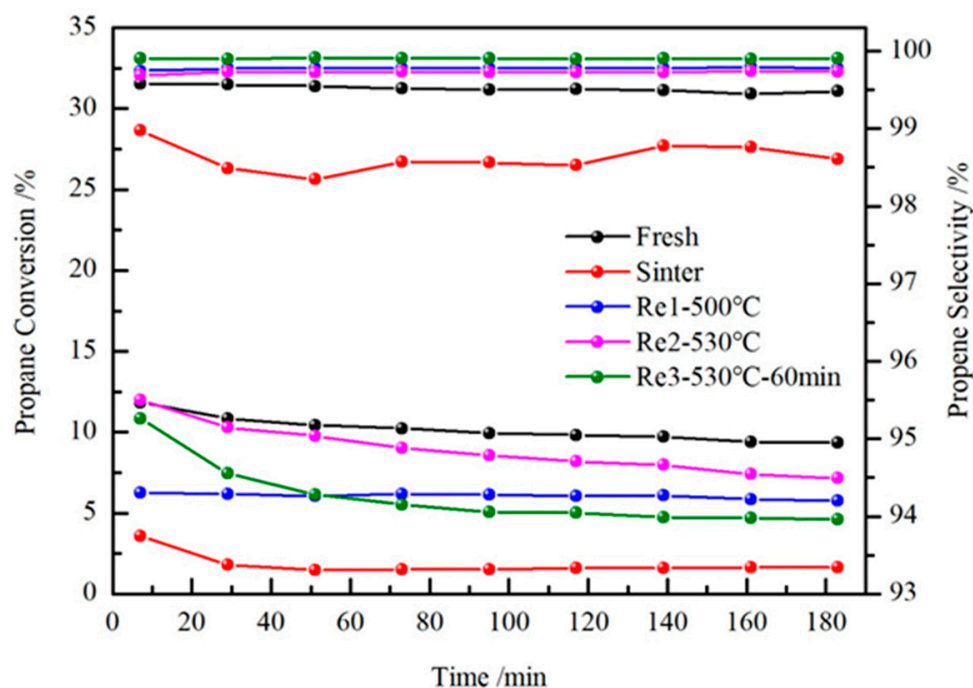


Figure 8. Regeneration performance of 700 °C oxidation catalyst.

3. Materials and Methods

The catalyst, PDC-20, was provided by Sino-Platinum Industrial Catalyst (Yunnan) Co., Ltd. (Yuxi, China), which comprised θ -Al₂O₃-supported 0.26 wt% Pt, 0.12 wt% Sn, and other promoters and in the shape of a sphere with a diameter of 1.2 mm. The received catalyst was crushed into particles with a size of less than 120 mesh and named Fresh. The Fresh catalyst was heated in a muffle furnace at a rate of 2 °C/min to setting temperature and calcined for 4 h; the obtained was named Sinter-*°C, where * indicated the oxidation temperature.

The oxychlorination treatment was conducted in an automatic micro-fixed bed reactor (μ BenchCat, Altamira Instruments, Cumming, GA, USA). The Sinter catalysts were loaded into the middle of the reactor and heated at a rate of 10 °C/min in a 30 mL/min argon

atmosphere to the target temperature. Then, an O₂/Ar mixed gas was introduced, and EDC was continuously added into the reactor. The typical oxychlorination conditions were as follows: temperature, 500 °C; O₂ concentration, 12%; EDC flow rate, 500 μmol/min; and regeneration time, 40 min. The regenerated catalyst samples are named Re-*°C, with the suffix indicating different oxidation temperatures. In Section 2.8, different oxychlorination conditions were adopted. Re1-500 °C was obtained under the same conditions as those for Re-*°C samples. Re2-530 °C was obtained by changing the oxychlorination temperature to 530 °C while other conditions remained. Increasing the regeneration time of a Re2-530 °C to 60 min would generate a Re2-530 °C 60 min sample.

The evaluation of the catalyst used the same reactor as described above. A 0.1 g catalyst was loaded and reduced in a hydrogen atmosphere at 550 °C for 100 min, followed by ramping the temperature up to 575 °C in an argon atmosphere. Subsequently, the reactor was switched to a mixture of C₃H₈, H₂, and Ar for the reaction, with a volume ratio of H₂/C₃H₈ = 0.8 (H₂ flow rate, 16 mL/min) and a total gas flow rate of 80 mL/min. The outlet products were analyzed by an online gas chromatograph.

The ASAP2020 instrument (Micromeritics, Norcross, GA, USA) was used for N₂ physisorption measurement to determine the textural properties of the catalysts. The AutoChem II (Micromeritics, Norcross, GA, USA) was used for CO chemisorption to characterize the dispersion of Pt in the catalysts. The D & advantage X-ray diffractometer (Cu Kα radiation, λ = 1.5406 Å, Bruker, Billerica, MA, USA) was used to characterize the crystalline structure of different catalysts. The Jem-2100F (JEOL Ltd., Musashino, Japan) was used for HAADF-STEM to characterize the distribution and particle size of Pt in the catalysts. Thermogravimetric analysis was carried out in a Pyris 1 instrument (PerkinElmer Instruments Co., Ltd., Waltham, MA, USA). The CO-DRIFTS spectrum was collected in a Spectrum 100 spectrometer (PerkinElmer, USA). An ESCALAB 250Xi spectrometer (Thermo Scientific, Waltham, MA, USA) was used for XPS characterization. The details of the operation can be referred to in the reference [28].

4. Conclusions

Oxychlorination regeneration of a commercial Pt-Sn/Al₂O₃ propane dehydrogenation catalyst oxidized at different temperatures was investigated. It was found that the oxidation temperature had a significant impact on the catalytic structure and performance of the regenerated catalyst. Above 550 °C, different oxidation temperatures resulted in different degrees of sintering of the catalyst. A severe aggregation of Pt and SnO_x was observed when the oxidation temperature reached 700 °C, and such a catalyst could not be regenerated under the same oxychlorination conditions as those for samples oxidized at lower temperatures. When the catalyst was oxidized below 650 °C, together with the aggregation of Pt, SnCl_x was transformed into quasi-metallic Sn species, and SnCl_x could be formed again in the following oxychlorination process to enhance the dispersion of Pt. When oxidized at 700 °C, more Sn was segregated and tended to exist in the Sn⁰ state, and the SnCl_x could not be formed in the oxychlorination and its promotion effect on Pt re-dispersion weakened. Although the catalytic performance could be fully restored after oxychlorination regeneration when the oxidation temperature was below 650 °C, their activity varies with oxidation temperature, possibly due to the change in Pt anchoring sites and surface properties of the support. This demanded that oxychlorination conditions should be tailored according to the precedent oxidation temperature to favorable redispersion kinetics. Lastly, the Pt-based catalyst deactivation caused by sintering is not irreversible when the oxidation temperature does not exceed 700 °C.

Author Contributions: C.Z.: investigation and writing—original draft preparation. M.T.: investigation. Z.S.: conceptualization, methodology, writing—review and editing, and funding acquisition. N.A.: resources and investigation. Y.S.: funding acquisition and writing—review and editing. X.Z.: resources and supervision. All authors have read and agreed to the published version of the manuscript.

Funding: This research was funded by the Natural Science Foundation of China, grant number 22278130, and the Foundation of Yunnan Province Science and Technology Department, grant number 202305AF150194.

Data Availability Statement: The data presented in this study are available in the article.

Conflicts of Interest: Nihong An and Yafeng Shen were employed by the Sino-Platinum Industrial Catalyst (Yunnan) Co., Ltd. The remaining authors declare that the research was conducted in the absence of any commercial or financial relationships that could be construed as a potential conflict of interest.

References

1. Dai, Y.; Gao, X.; Wang, Q.; Wan, X.; Zhou, C.; Yang, Y. Recent progress in heterogeneous metal and metal oxide catalysts for direct dehydrogenation of ethane and propane. *Chem. Soc. Rev.* **2021**, *50*, 5590–5630. [[CrossRef](#)] [[PubMed](#)]
2. Sun, M.; Zhai, S.; Weng, C.; Wang, H.; Yuan, Z.-Y. Pt-based catalysts for direct propane dehydrogenation: Mechanisms revelation, advanced design, and challenges. *Mol. Catal.* **2024**, *558*, 114029. [[CrossRef](#)]
3. Sattler, J.J.H.B.; Ruiz-Martinez, J.; Santillan-Jimenez, E.; Weckhuysen, B.M. Catalytic Dehydrogenation of Light Alkanes on Metals and Metal Oxides. *Chem. Rev.* **2014**, *114*, 10613–10653. [[CrossRef](#)] [[PubMed](#)]
4. Zhang, X.P.; Sui, Z.J.; Zhou, X.G.; Yuan, W.K. Modeling and Simulation of Coke Combustion Regeneration for Coked Cr₂O₃/Al₂O₃ Propane Dehydrogenation Catalyst. *Chin. J. Chem. Eng.* **2010**, *18*, 618–625.
5. Otroshchenko, T.; Jiang, G.; Kondratenko, V.A.; Rodemerck, U.; Kondratenko, E.V. Current status and perspectives in oxidative, non-oxidative and CO₂-mediated dehydrogenation of propane and isobutane over metal oxide catalysts. *Chem. Soc. Rev.* **2021**, *50*, 473–527. [[CrossRef](#)] [[PubMed](#)]
6. Dai, Y.; Lu, P.; Cao, Z.; Campbell, C.T.; Xia, Y. The physical chemistry and materials science behind sinter-resistant catalysts. *Chem. Soc. Rev.* **2018**, *47*, 4314–4331. [[CrossRef](#)] [[PubMed](#)]
7. Shi, L.; Deng, G.-M.; Li, W.-C.; Miao, S.; Wang, Q.-N.; Zhang, W.-P.; Lu, A.-H. Al₂O₃ Nanosheets Rich in Pentacoordinate Al³⁺ Ions Stabilize Pt-Sn Clusters for Propane Dehydrogenation. *Angew. Chem. Int. Ed.* **2015**, *54*, 13994–13998. [[CrossRef](#)] [[PubMed](#)]
8. Mironenko, R.M.; Belskaya, O.B.; Talsi, V.P.; Gulyaeva, T.I.; Kazakov, M.O.; Nizovskii, A.I.; Kalinkin, A.V.; Bukhtiyarov, V.I.; Lavrenov, A.V.; Likholobov, V.A. Effect of γ -Al₂O₃ hydrothermal treatment on the formation and properties of platinum sites in Pt/ γ -Al₂O₃ catalysts. *Appl. Catal. A Gen.* **2014**, *469*, 472–482. [[CrossRef](#)]
9. Liu, Y.; Zong, X.; Patra, A.; Caratzoulas, S.; Vlachos, D.G. Propane Dehydrogenation on Pt_xSn_y (x, y \leq 4) Clusters on Al₂O₃(110). *ACS Catal.* **2023**, *13*, 2802–2812. [[CrossRef](#)]
10. Zhang, Y.W.; Zhou, Y.M.; Tang, M.H.; Liu, X.; Duan, Y.Z. Effect of La calcination temperature on catalytic performance of PtSnNaLa/ZSM-5 catalyst for propane dehydrogenation. *Chem. Eng. J.* **2012**, *181*, 530–537. [[CrossRef](#)]
11. Ma, Z.H.; Wang, J.; Li, J.; Wang, N.N.; An, C.H.; Sun, L.Y. Propane dehydrogenation over Al₂O₃ supported Pt nanoparticles: Effect of cerium addition. *Fuel Process. Technol.* **2014**, *128*, 283–288. [[CrossRef](#)]
12. Im, J.; Choi, M. Physicochemical Stabilization of Pt against Sintering for a Dehydrogenation Catalyst with High Activity, Selectivity, and Durability. *ACS Catal.* **2016**, *6*, 2819–2826. [[CrossRef](#)]
13. Long, L.L.; Lang, W.Z.; Yan, X.; Xia, K.; Guo, Y.J. Yttrium-modified alumina as support for trimetallic PtSnIn catalysts with improved catalytic performance in propane dehydrogenation. *Fuel Process. Technol.* **2016**, *146*, 48–55. [[CrossRef](#)]
14. Kwon, H.C.; Park, Y.; Park, J.Y.; Ryoo, R.; Shin, H.; Choi, M. Catalytic Interplay of Ga, Pt, and Ce on the Alumina Surface Enabling High Activity, Selectivity, and Stability in Propane Dehydrogenation. *ACS Catal.* **2021**, *11*, 10767–10777. [[CrossRef](#)]
15. Zhang, W.; Lei, J.; Sui, Z.-J.; Zhu, K.-K.; Zhu, Y.-A.; Zhou, X.-G. Thermal stability of nanoparticle supported on Al₂O₃ with different morphologies. *Mater. Res. Express* **2019**, *6*, 095064. [[CrossRef](#)]
16. Monzón, A.; Garetto, T.F.; Borgna, A. Sintering and redispersion of Pt/ γ -Al₂O₃ catalysts: A kinetic model. *Appl. Catal. A Gen.* **2003**, *248*, 279–289. [[CrossRef](#)]
17. Fiedorow, R.M.J.; Wanke, S.E. The sintering of supported metal catalysts: I. Redispersion of supported platinum in oxygen. *J. Catal.* **1976**, *43*, 34–42. [[CrossRef](#)]
18. Alcalá, R.; Dean, D.P.; Chavan, I.; Chang, C.-W.; Burnside, B.; Pham, H.N.; Peterson, E.; Miller, J.T.; Datye, A.K. Strategies for regeneration of Pt-alloy catalysts supported on silica for propane dehydrogenation. *Appl. Catal. A Gen.* **2023**, *658*, 119157. [[CrossRef](#)]
19. Gao, X.-Q.; Yao, Z.-H.; Li, W.-C.; Deng, G.-M.; He, L.; Si, R.; Wang, J.-G.; Lu, A.-H. Calcium-Modified PtSn/Al₂O₃ Catalyst for Propane Dehydrogenation with High Activity and Stability. *Chemcatchem* **2023**, *15*, e202201691. [[CrossRef](#)]
20. Zhu, X.; Wang, T.; Xu, Z.; Yue, Y.; Lin, M.; Zhu, H. Pt-Sn clusters anchored at Al³⁺ sites as a sinter-resistant and regenerable catalyst for propane dehydrogenation. *J. Energy Chem.* **2022**, *65*, 293–301. [[CrossRef](#)]
21. Bournonville, J.P.; Franck, J.P.; Martino, G. Influence of the Various Activation Steps on the Dispersion and the Catalytic Properties of Platinum Supported on Chlorinated Alumina. In *Studies in Surface Science and Catalysis*; Poncelet, G., Grange, P., Jacobs, P.A., Eds.; Elsevier: Amsterdam, The Netherlands, 1983; Volume 16, pp. 81–90.

22. Deng, S.; Qiu, C.; Yao, Z.; Sun, X.; Wei, Z.; Zhuang, G.; Zhong, X.; Wang, J.-G. Multiscale simulation on thermal stability of supported metal nanocatalysts. *Wiley Interdiscip. Rev. Comput. Mol. Sci.* **2019**, *9*, e1405. [[CrossRef](#)]
23. Zhao, F.-C.; Yang, H.; Sui, Z.-J.; Zhu, Y.-A.; Chen, D.; Zhou, X.-G. Self-adaptive structure and catalytic performance of the Pt-Sn/Al₂O₃ propane dehydrogenation catalyst regenerated by dichloroethane oxychlorination. *Catal. Sci. Technol.* **2022**, *12*, 7171–7181. [[CrossRef](#)]
24. Yang, Y.; Miao, C.; Wang, R.; Zhang, R.; Li, X.; Wang, J.; Wang, X.; Yao, J. Advances in morphology-controlled alumina and its supported Pd catalysts: Synthesis and applications. *Chem. Soc. Rev.* **2024**, *53*, 5014–5053. [[CrossRef](#)] [[PubMed](#)]
25. Morgan, K.; Goguet, A.; Hardacre, C. Metal Redispersion Strategies for Recycling of Supported Metal Catalysts: A Perspective. *ACS Catal.* **2015**, *5*, 3430–3445. [[CrossRef](#)]
26. Choi, Y.S.; Oh, K.; Jung, K.-D.; Kim, W.-I.; Koh, H.L. Regeneration of Pt-Sn/Al₂O₃ Catalyst for Hydrogen Production through Propane Dehydrogenation Using Hydrochloric Acid. *Catalysts* **2020**, *10*, 898. [[CrossRef](#)]
27. Ren, G.; Xiong, S.; Li, X.; Lai, X.; Chen, J.; Chu, M.; Xu, Y.; Huang, S. Regeneration of sintered platinum at mild temperature for propane dehydrogenation. *J. Catal.* **2024**, *429*, 115276. [[CrossRef](#)]
28. Dong, L.; Sun, Y.; Zhou, Y.; Sui, Z.; Dai, Y.; Zhu, Y.; Zhou, X. Structure Robustness of Highly Dispersed Pt/Al₂O₃ Catalyst for Propane Dehydrogenation during Oxychlorination Regeneration Process. *Catalysts* **2024**, *14*, 48. [[CrossRef](#)]
29. Ouyang, R.; Liu, J.-X.; Li, W.-X. Atomistic Theory of Ostwald Ripening and Disintegration of Supported Metal Particles under Reaction Conditions. *J. Am. Chem. Soc.* **2013**, *135*, 1760–1771. [[CrossRef](#)] [[PubMed](#)]
30. Wang, H.-Z.; Sun, L.-L.; Sui, Z.-J.; Zhu, Y.-A.; Ye, G.-H.; Chen, D.; Zhou, X.-G.; Yuan, W.-K. Coke Formation on Pt-Sn/Al₂O₃ Catalyst for Propane Dehydrogenation. *Ind. Eng. Chem. Res.* **2018**, *57*, 8647–8654. [[CrossRef](#)]
31. Zhang, W.; Wang, H.; Jiang, J.; Sui, Z.; Zhu, Y.; Chen, D.; Zhou, X. Size Dependence of Pt Catalysts for Propane Dehydrogenation: From Atomically Dispersed to Nanoparticles. *ACS Catal.* **2020**, *10*, 12932–12942. [[CrossRef](#)]
32. Choi, Y.S.; Kim, J.-R.; Hwang, J.-H.; Roh, H.-S.; Koh, H.L. Effect of reduction temperature on the activity of Pt-Sn/Al₂O₃ catalysts for propane dehydrogenation. *Catal. Today* **2023**, *411*, 113957. [[CrossRef](#)]
33. He, S.B.; Sun, C.L.; Bai, Z.W.; Dai, X.H.; Wang, B. Dehydrogenation of long chain paraffins over supported Pt-Sn-K/Al₂O₃ catalysts: A study of the alumina support effect. *Appl. Catal. A Gen.* **2009**, *356*, 88–98. [[CrossRef](#)]
34. Lieske, H.; Lietz, G.; Spindler, H.; Völter, J. Reactions of platinum in oxygen- and hydrogen-treated Pt γ -Al₂O₃ catalysts: I. Temperature-programmed reduction, adsorption, and redispersion of platinum. *J. Catal.* **1983**, *81*, 8–16. [[CrossRef](#)]
35. Padró, C.L.; de Miguel, S.R.; Castro, A.A.; Scelza, O.A. Stability and regeneration of supported PtSn catalysts for propane dehydrogenation. In *Studies in Surface Science and Catalysis*; Bartholomew, C.H., Fuentes, G.A., Eds.; Elsevier: Amsterdam, The Netherlands, 1997; Volume 111, pp. 191–198.
36. Shi, Y.; Li, X.; Rong, X.; Gu, B.; Wei, H.; Zhao, Y.; Wang, W.; Sun, C. Effect of Aging Temperature of Support on Catalytic Performance of PtSnK/Al₂O₃ Propane Dehydrogenation Catalyst. *Catal. Lett.* **2020**, *150*, 2283–2293. [[CrossRef](#)]
37. Borges, L.R.; da Silva, A.G.M.; Braga, A.H.; Rossi, L.M.; Suller Garcia, M.A.; Vidinha, P. Towards the Effect of Pt⁰/Pt ^{δ} and Ce³⁺ Species at the Surface of CeO₂ Crystals: Understanding the Nature of the Interactions under CO Oxidation Conditions. *Chemcatchem* **2021**, *13*, 1340–1354. [[CrossRef](#)]
38. Shan, Y.; Sui, Z.; Zhu, Y.; Chen, D.; Zhou, X. Effect of steam addition on the structure and activity of Pt-Sn catalysts in propane dehydrogenation. *Chem. Eng. J.* **2015**, *278*, 240–248. [[CrossRef](#)]
39. Virnovskaia, A.; Morandi, S.; Rytter, E.; Ghiotti, G.; Olsbye, U. Characterization of PtSn/Mg(Al)O catalysts for light alkane dehydrogenation by FT-IR Spectroscopy and catalytic measurements. *J. Phys. Chem. C* **2007**, *111*, 14732–14742. [[CrossRef](#)]
40. Pham, H.N.; Sattler, J.J.H.B.; Weckhuysen, B.M.; Datye, A.K. Role of Sn in the Regeneration of Pt/ γ -Al₂O₃ Light Alkane Dehydrogenation Catalysts. *ACS Catal.* **2016**, *6*, 2257–2264. [[CrossRef](#)]
41. Afonso, J.C.; Aranda, D.A.G.; Schmal, M.; Frety, R. Regeneration of a Pt SnAl₂O₃ catalyst: Influence of heating rate, temperature and time of regeneration. *Fuel Process. Technol.* **1997**, *50*, 35–48. [[CrossRef](#)]
42. Le Normand, F.; Borgna, A.; Garetto, T.F.; Apesteguia, C.R.; Moraweck, B. Redispersion of Sintered Pt/Al₂O₃ Naphtha Reforming Catalysts: An in Situ Study Monitored by X-ray Absorption Spectroscopy. *J. Phys. Chem.* **1996**, *100*, 9068–9076. [[CrossRef](#)]
43. Gracia, F.J.; Miller, J.T.; Kropf, A.J.; Wolf, E.E. Kinetics, FTIR, and Controlled Atmosphere EXAFS Study of the Effect of Chlorine on Pt-Supported Catalysts during Oxidation Reactions. *J. Catal.* **2002**, *209*, 341–354. [[CrossRef](#)]
44. Kamiuchi, N.; Taguchi, K.; Matsui, T.; Kikuchi, R.; Eguchi, K. Sintering and redispersion of platinum catalysts supported on tin oxide. *Appl. Catal. B Environ.* **2009**, *89*, 65–72. [[CrossRef](#)]
45. Serrano-Ruiz, J.C.; Sepúlveda-Escribano, A.; Rodríguez-Reinoso, F. Bimetallic PtSn/C catalysts promoted by ceria: Application in the nonoxidative dehydrogenation of isobutane. *J. Catal.* **2007**, *246*, 158–165. [[CrossRef](#)]
46. Kim, G.H.; Jung, K.-D.; Kim, W.-I.; Um, B.-H.; Shin, C.-H.; Oh, K.; Koh, H.L. Effect of oxychlorination treatment on the regeneration of Pt-Sn/Al₂O₃ catalyst for propane dehydrogenation. *Res. Chem. Intermed.* **2016**, *42*, 351–365. [[CrossRef](#)]
47. Shi, Y.; Li, X.R.; Rong, X.; Gu, B.; Wei, H.Z.; Sun, C.L. Influence of support on the catalytic properties of Pt-Sn-K/ θ -Al₂O₃ for propane dehydrogenation. *RSC Adv.* **2017**, *7*, 19841–19848. [[CrossRef](#)]

48. Virnovskaia, A.; Jorgensen, S.; Hafizovic, J.; Prytz, O.; Kleimenov, E.; Havecker, M.; Bluhm, H.; Knop-Gericke, A.; Schlogl, R.; Olsbye, U. In situ XPS investigation of Pt(Sn)/Mg(Al)O catalysts during ethane dehydrogenation experiments. *Surf. Sci.* **2007**, *601*, 30–43. [[CrossRef](#)]
49. Ma, Y.; Chen, X.; Guan, Y.J.; Xu, H.; Zhang, J.W.; Jiang, J.G.; Chen, L.; Xue, T.; Xue, Q.S.; Wei, F.; et al. Skeleton-Sn anchoring isolated Pt site to confine subnanometric clusters within *BEA topology. *J. Catal.* **2021**, *397*, 44–57. [[CrossRef](#)]

Disclaimer/Publisher’s Note: The statements, opinions and data contained in all publications are solely those of the individual author(s) and contributor(s) and not of MDPI and/or the editor(s). MDPI and/or the editor(s) disclaim responsibility for any injury to people or property resulting from any ideas, methods, instructions or products referred to in the content.